Cost-Optimal Security-Constrained Control for a Smart Marina Facility

F. Conte
Università Campus Bio-Medico di Roma
Faculty of Engineering
Via Alvaro del Portillo, 21
I-00128, Roma, Italy
f.conte@unicampus.it

F. D'Agostino, M. Gallo, F. Graffione, G. Natrella, F. Silvestro
University of Genova
DITEN
Via all'Opera Pia 11 A
I-16145, Genova, Italy
federico.silvestro@unige.it

***Abstract*—This work presents an optimal management strategy for a smart marina facility, designed to coordinate multiple onshore energy resources while ensuring the secure operation of the port's electrical distribution network. The proposed approach integrates renewable energy resources, battery energy storage, and a set of electric charging infrastructures serving both vessels and land-based vehicles. A model predictive control based approach is proposed to control generating units and define the charging schedule of connected rechargeable units, while ensuring that voltage and current operational limits are respected. The methodology is validated through simulations based on the real operating conditions of the marina of Finale Ligure, Italy, demonstrating its capability to provide efficient, feasible and secure operation under realistic scenarios.**

***Index Terms*—Smart Port, Shore Charging, Voltage Regulation, Electrical Vehicles, Electrical Ships**

I. Introduction

In the maritime sector, ports serve as a crucial interface between vessels and onshore infrastructures. As the use of Electric Ships (ESs), Electric Vehicles (EVs), and Renewable Energy Sources (RESs) rapidly increases, port power systems are facing new operational challenges. These trends, combined with evolving environmental regulations and the rise of cold-ironing infrastructures, have made the design and operation of sustainable and efficient port energy systems a central priority. As a result, the concepts of Smart Ports and digitalization have gained strategic importance [1], [2].

The increasing number of electrical loads and energy resources installed in ports is making their power distribution networks significantly more complex to operate. Properly accounting for the electrical constraints of the distribution system is therefore essential. While the connection to the national grid ensures overall system stability and regulation capabilities, several ancillary services can be provided within the local port subnet. These include voltage regulation through reactive power injection and the control of power flows between nodes to avoid local congestion and thermal overloads.

Funded by the European Union - NextGenerationEU and by the Ministry of University and Research (MUR), National Recovery and Resilience Plan (NRRP), Mission 4, Component 2, Investment 1.5, project "RAISE - Robotics and AI for Socio-economic Empowerment" (ECS00000035).

Integrating these functionalities into an overall energy management strategy has shown promising results in port applications. In the literature, several different solutions have been proposed by various authors. In [3], the authors propose an optimal management approach for a port's integrated energy system that leverages demand response to lower operating costs. In [4], a methodology is developed to model EV charging loads while accounting for stochastic factors, and to assess their impact on distribution systems under different scenarios. In [5], an energy optimal scheduling method for the multi-energy integration system in ports is described, focusing on carbon emission reduction. In [6], a distributed energy management approach for large ports is proposed, based on an alternating direction method of multipliers algorithm.

In most of the literature, operational security constraints are not taken into account in the development of smart port management control methods. This paper proposes a Model Predictive Control (MPC) based strategy to control the resources installed in a real smart marina facility located in Italy, including on-shore Recharge Stations (RSs) both for ESs and EVs, one Battery Energy Storage System (BESS), one Hydrogen Energy Storage System (HESS), and RESs. While minimizing the operational energy costs, the proposed algorithm ensures that voltage and line current security constraints are not violated. Simulation results validate the approach.

II. Case Study

This paper considers the real-world case study located in the Smart Marina of Finale Ligure (Savona, Italy). The port is already equipped with RS for ES, and an executive project to be completed by December 2025 includes the installation of RES generation units, BESSs, and additional RSs for both EVs and ESs. In the following years, further components will be deployed as part of a broader initiative to develop a green port pilot within this touristic area.

A. Layout of the Marina Grid

The layout of the marina 400V LV grid is shown in Fig. 1. The rated power import from the utility grid is 130 kW. The marina serves different classes of Rechargeable Units (RUs): EVs, subdivided into small EVs (SEVs) and heavy

979-8-3315-8138-1

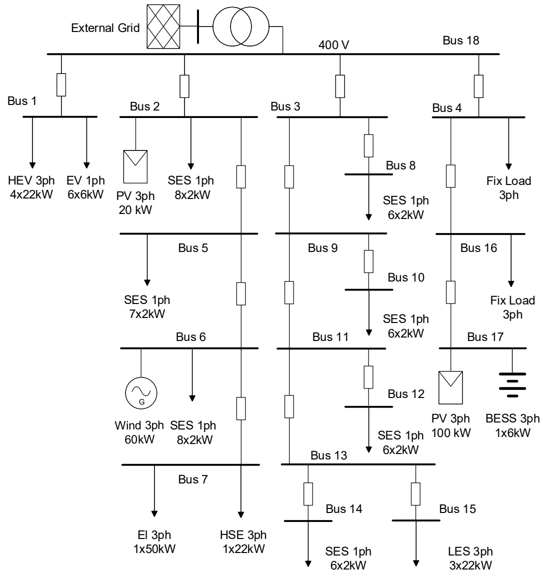

Fig. 1. Layout of the marina LV distribution grid.

EVs (HEVs); ESs, subdivided into small ESs (SESs) and large ESs (LESs); and Hydrogen-hybrid Ships (HSs), equipped with on-board fuel cells and auxiliary batteries. Fig. 1 shows the number and nominal power of each installed RS. Note that there is only one RS for HSs, located at bus 7 and labeled HSE. The figure also indicates whether each RS is single-phase or three-phase connected.

Other than the RUs, the port is equipped with: Photovoltaics (PVs) at buses 2 and 17, a wind farm at bus 6, two fix loads at buses 4 and 16, representing buildings, a BESS at bus 17 and HESS composed of an Electrolyzer (El) and a Hydrogen Tank (HT) at bus 7. Nominal powers are all reported Fig. 1.

B. Users Demand Scenarios

The demands of the RUs are generated randomly according to the expected number of arrivals per day per RS na_u, the number of RSs, the size of the units, and the time of stay (a random number in the interval ΔT_u). Specifically, for each type of RUs, a group of categories is individuated through an upper and a lower capacity, *i.e.*, uc_u, lc_u. The size of the RUs C^u_{nom}, their arrival charge level and their desired level of charge at departure $\hat{C}^u$, are generated randomly: the first one in the interval $[lc_u, uc_u]$, the second one in the interval $[0, C^u_{nom}/2]$, and the third one as a random increase, feasible with the specifications of the corresponding RSs, time of stay, and C^u_{nom}. The details are given in Table I. Notice that the equivalent energy demand of HSs is calculated on lower heating value basis, considering a 55% efficiency from hydrogen to the shaft of the HS.

III. Models

This section introduces the models used by the MPC algorithm presented in the next section. All models are formulated in discrete time; t denotes the timestamp, and the sampling interval is $\Delta t = 15$ min.

TABLE I
DETAILS OF RECHARGEABLE UNITS DEMAND SCENARIOS

RU	EV	HEV	LES	SES	HSE	HS
na_u	3	3	2	2	1	1
ΔT_u [h]	[1,8]	[1,8]	[2,18]	[2,18]	[2,18]	[2,18]
$[lc_u, uc_u]$ [kWh] [kg] for HS	[3,8] [16,30] [30,50] [50,75]	[50,75] [75,120] [120,150]	[20,40] [40,80] [80,150] [150,250]	[2,5] [5,10] [10,20]	[15,25] [25,40] [40,80]	[100,150] [150,200] [200,300]

A. Rechargeable Units Model

As described in Section II, the marina serves different classes of RUs. It is assumed that the control algorithm has no advance knowledge about the connection times of these units and of their energy demand. However, the underlying hypothesis is that, once a RU u is connected, it communicates its current charge C^u_t, its departure time $\hat{T}_u$, and its desired final charge $\hat{C}^u$. The generic connected RU $u \in \mathcal{RU}$ is therefore modeled as follows:

$$C^u_{t+1} = C^u_t + \Delta t \cdot \eta^u P^u_t \quad (1)$$

$$\hat{C}^u \leq C^u_{\hat{T}_u} \leq C^u_{nom} \quad (2)$$

$$0 \leq P^u_t \leq P^u_{nom} \quad (3)$$

where C^u_{nom} is the nominal capacity, η^u is the charge efficiency, P^u_t and P^u_{nom} are the charging power of the RS where the RU is connected and its rated value, respectively.

Model (1)–(3) is defined for EVs, ESs and HSs. However, by being hybrid, the HS has a dual demand: hydrogen demand P^{hs}_t, which is served by connecting to the shore HT, and electrical power demand P^{hse}_t to charge the on board auxiliary batteries. Thus, model (1)–(3) is defined both for $u = hs, hse$.

B. Storage Systems Models

The BESS and HESS are modeled as follows:

$$0 \leq P^{ch}_t \leq P^b_{nom} \delta^b_t, \quad (4)$$

$$0 \leq P^{ds}_t \leq P^b_{nom} \left(1 - \delta^b_t\right), \quad (5)$$

$$S_{t+1} = S_t + \frac{\Delta t}{E^b} \left(\eta^{ch} P^{ch}_t - \frac{P^{ds}_t}{\eta^{ds}} \right), \quad (6)$$

$$\underline{S} \leq S_t \leq \overline{S}, \quad (7)$$

$$P^{el}_{min} \delta^{el}_t \leq P^{el}_t \leq P^{el}_{nom} \delta^{el}_t, \quad (8)$$

$$H_{t+1} = H_t + \frac{\Delta t}{E^h} \left(\eta^{el} P^{el}_t - \sum_{\ell} P^{hs,\ell}_t \right), \quad (9)$$

$$\underline{H} \leq H_t \leq \overline{H}, \quad (10)$$

where: P^{ch}_t, P^{ds}_t and P^b_{nom} are the BESS charge, discharge and nominal powers, respectively; η^{ch} and η^{ds} are the BESS charge and discharge efficiencies, respectively; S_t, $\underline{S}$ and $\overline{S}$ are the BESS State of Charge (SoC) and its lower and upper limits, respectively; E^b is the BESS capacity; P^{el}_t, P^{el}_{min} and P^{el}_{nom} are the El power and its lower and upper limits, respectively; η^{el} is the El efficiency; H_t, $\underline{H}$ and $\overline{H}$ are the HT Level of Hydrogen (LoH) and its lower and upper limits, respectively; E^h is the HT capacity.

979-8-3315-8138-1

C. Renewable generation units

The marina is equipped with two PVs plants and three Wind Turbines (WTs). The control algorithm is supposed to be provided with the generation forecasts $\hat{P}_t^{pv}$ and $\hat{P}_t^{w}$. The control algorithm can decide to apply any curtailment, meaning that, for all RES generation units u:

$$P_t^u \leq \hat{P}_t^u \tag{11}$$

D. Marina Grid Model

The marina LV grid is modeled using the approach introduced in [7], [8] for distribution networks. Let be: V_k the voltage phasor (p.u.) and I_k the current injection phasor at bus $k \in \{1, 2, \dots, N\}$ at any timestamp t (symbol omitted in this subsection). As proposed in [7], [8], starting from the ZIP model, the relation between I_k and V_k can be linearized around the nominal voltage to obtain:

$$I_k = S_{P,k}^* \cdot (2 - V_k^*) + I_{C,k} + Z_k^* \cdot V_k \tag{12}$$

where $S_{P,k}$ is the constant power, $I_{C,k}$ is the constant current and Z_k is the constant impedance. Let us consider the admittance matrix in the form:

$$\begin{bmatrix} I_s \\ I_N \end{bmatrix} = \begin{bmatrix} Y_{ss} & Y_{sN} \\ Y_{Ns} & Y_{NN} \end{bmatrix} \begin{bmatrix} V_s \\ V_N \end{bmatrix} \tag{13}$$

where s indicate the slack bus (point of connection with the MV grid in the case study) and N indicates the set of the remaining buses. Using (12) and (13), the network equations can be expressed with the following linear form:

$$I_{C,N} = A + BV_N^* + CV_N \tag{14}$$
$$I_s = Y_{ss}V_s + Y_{sN}V_N \tag{15}$$

where $A = Y_{Ns}V_s - 2S_{P,N}^*$, $B = diag(S_{P,N}^*)$, and $C = Y_{NN} - diag(Z_N^*)$. Notice that constant current components of the bus current injections $I_{C,N}$ have been left explicit in the network equations (14) since they are considered as control variables, as better explained below.

Assuming the slack voltage $V_s = 1e^{j0}$ and a reasonable angle range $-3° < \delta < 3°$, voltage limits can be expressed in Cartesian form:

$$0.95 \leq V_k^{\mathrm{re}} \leq 1.05 \tag{16}$$
$$-0.05 \leq V_k^{\mathrm{im}} \leq 0.05 \tag{17}$$

Lines currents I_l, $l \in \{1, \dots, L\}$ can be computed by:

$$V_h^{\mathrm{re}} - V_k^{\mathrm{re}} = R_l I_l^{\mathrm{re}} - X_l I_l^{\mathrm{im}} \tag{18}$$
$$V_h^{\mathrm{im}} - V_k^{\mathrm{im}} = X_l I_b^{\mathrm{re}} + R_l I_l^{\mathrm{im}} \tag{19}$$

where R_l and X_l are the lines resistance and reactance, respectively.

The maximal line current constrains are defined as in [8] to obtain the linear formulation:

$$-I_l^{\max} \leq I_l^{\mathrm{re}} \leq I_l^{\max} \tag{20}$$
$$-I_l^{\max} \leq I_l^{\mathrm{im}} \leq I_l^{\max} \tag{21}$$
$$-\sqrt{2}\, I_l^{\max} \leq I_l^{\mathrm{im}} \pm I_l^{\mathrm{re}} \leq \sqrt{2}\, I_l^{\max} \tag{22}$$

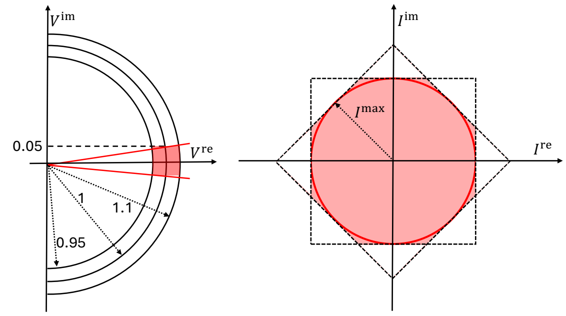

Fig. 2. Bus voltage and line current limits designed by constraints (16)–(17) and (20)–(22).

where I_l^{max} is the rated current of line l.

Fig. 2 shows how the constraints (16)–(17) and (20)–(22) define the voltage and line currents limits.

Constraints of the same form as (20)–(22) are finally applied to the slack current I_s, with $I_s^{\max}$ being the maximum current that can be imported from the utility grid.

E. Unit connections

In this work, the control variables are the active and reactive power set-points of all RUs, BESS, HESS, PVs and WTs.

As described in Section II, some RUs have a three-phase connection, while others have a single-phase connection. Therefore, the grid model proposed in Section III-D must be adapted to handle the unbalanced case.

The mutual coupling among phases are neglected and it is assumed that all three-phase units are balanced and star-connected. Consequently, the same model (14)–(15) and constraints (16)–(22) can be applied to each of the three phases, with V_k^p, $p \in a, b, c$ denoting the phase-to-neutral voltages and the currents correspond to the single-phase values.

As introduced in [8], all controllable units are modeled as constant current sources/loads. Thus, connection of units with the grid is modeled in the following way. Let $I_{u,t}$ be the phasor of the current exchanged by unit u at time t. If a single-phase unit u is connected to the phase $p \in \{a, b, c\}$ of bus k, $I_{u,t}$ is added to the constant current injection $I_{C,k,t}^p$; if the a three-phase unit u is connected to bus k, current $I_{u,t}/3$ is added to all the constant phase current injections $I_{C,k,t}^p$, $p = \{a, b, c\}$.

As mentioned before, all units are supposed to be controlled by active and reactive power set-points P_t^u and Q_t^u, with $P_t^u > 0, Q_t^u > 0$ meaning consumption for load units (EVs, ESs, HSs, El and BESS charge) and injection for generation units (PVs, WTs and BESS discharge). Assuming that constraints (16)–(17) are always satisfied, the following approximation is adopted (considering $V_{k,t}^{\mathrm{re}} \approx 1$ and $V_{k,t}^{\mathrm{im}} \approx 0$):

$$P_t^u = \pm I_{u,t}^{\mathrm{re}} \qquad Q_t^u = \pm I_{u,t}^{\mathrm{im}} \tag{23}$$

with the plus sign for generation units and the minus one for load units. Given this approximation for active powers, (1)–(11) can be expressed in terms of $I_{u,t}^{\mathrm{re}}$ keeping the linearity of models.

979-8-3315-8138-1

Reactive power set-points must be limited according to the unit capabilities, assumed to be square. Therefore, the following constraints must hold for all units u:

$$-P^u_{nom} \leq I^{\text{im}}_{u,t} \leq P^u_{nom} \tag{24}$$

Finally, the case study considers two buildings treated as non-controllable loads, characterized by active and reactive power consumption P^l_t and Q^l_t. Both buildings are three-phase connected. Therefore, they are modeled as constant power loads by adding $-P^l_t/3 - j \cdot Q^l_t/3$ to $S^p_{P,t}$ for each phase $p \in \{a, b, c\}$.

IV. Control Algorithm

The control algorithm aims to minimize the marina electricity bill while simultaneously meeting the RUs demands, reducing the curtailment of RESs generation, maintaining voltages within safe limits, and preventing cable overloading.

The proposed control strategy is based on the MPC technique, in which, at each discrete timestamp, an appropriately defined optimization problem is solved over a finite prediction horizon T. Only the first element of the resulting control trajectory is applied, and the entire procedure is repeated at the subsequent timestamp.

At any timestamp t, given: the measurements of C^u_t, $C_{\hat{T}_u}$ for all connected RUs, S_t and H_t, and the forecasts of RES generation $\hat{P}^u_\tau$ and non-controllable loads $(\hat{P}^l_\tau, \hat{Q}^l_\tau)$ $\tau = t, t+1, \ldots, T-1$, the MPC optimization problem is:

$$\{P^{u*}_\tau, Q^{u*}_\tau\} = \arg\min \sum_{\tau=t}^{T-1} \gamma_\tau \left(-I^{\text{re}}_{s,\tau} + \alpha \sum_{u \in \mathcal{RU}} I^{\text{re}}_{u,\tau} \right) \tag{25}$$

such that, $\forall \tau = t, t+1, \ldots, T-1$: (1)–(3) hold true for all connected RUs $u \in \mathcal{RU}$, (4)–(10) hold true for BESS and HESS, (11) holds true for all RES generation units, (23)–(24) hold true for all controllable units u, (14)–(22) hold true for all phases $p = \{a, b, c\}$. Constant current and power components $I^p_{C,k,\tau}$ and $S^p_{P,k,t}$ in (14)–(22) are computed from unit currents $I_{u,t}$ and load forecasts $(\hat{P}^l_\tau, \hat{Q}^l_\tau)$ as detailed in Section III-E.

In (25), γ_τ represents the cost of electricity imported from the utility grid, whereas the coefficient $\alpha > 1$ models the income received by the marina for the recharge services. The latter term can, of course, be modeled differently depending on the actual tariff scheme applied.

It is worth noting that, since controllable units are operated according to the optimal active and reactive power set-points P^{u*}_t, Q^{u*}_t, no approximation error is introduced in the recharge of RUs, as the service to marina users is treated as a priority. Approximation errors only affect voltages and currents; however, our preliminary results indicate that the achieved accuracy is sufficient to ensure safe operating conditions.

V. Results

The control algorithm is tested over a three-day simulation, run in the MATLAB environment. MPC optimization problems are implemented with the Python library Pyomo and solved by Gurobi. Actual voltages and currents are computed using standard Newton–Raphson solutions of the nonlinear power-flow equations.

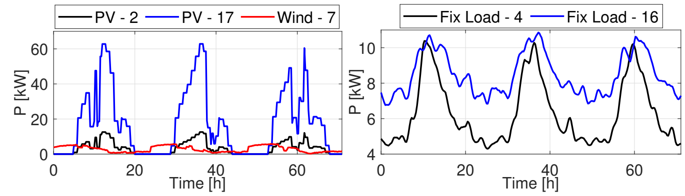

Fig. 3. Renewable energy generation and fix loads profiles.

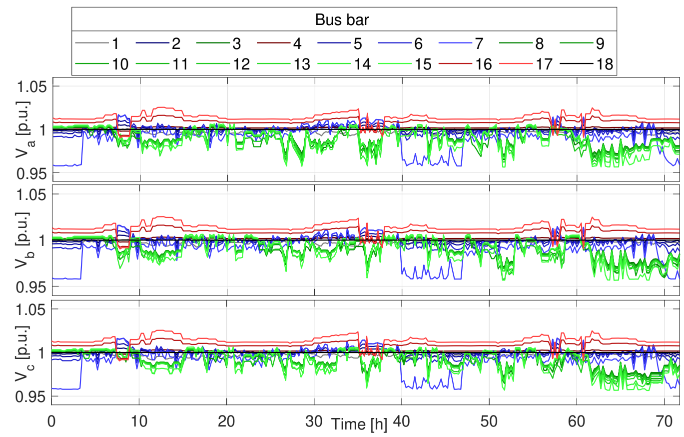

Fig. 4. Three-phase voltage amplitudes.

Fig. 3 shows RES generation and fix loads profiles for the three days of simulations. Fig. 4 depicts the obtained voltage amplitudes. Bus 7, hosting the El and the HSE, together with buses 14 and 15 are the most critic, however the voltage always remains in the prescribed limits. Fig. 5 shows the current load on lines. Notice that lines 6-7 and 3-18 are significantly loaded (dashed in the figure). Line 3-18 connects the connection with the utility grid to the feeder with the higher number of RUs, whereas line 6-7 connects the bus hosting the WTs with the bus hosting El and HSE. In any case, as shown in Fig. 5, the line ratings are never exceeded.

Fig. 6 shows the profiles of: storages charge levels, powers exchanged by BESS and El, number and type of connected RUs, and the aggregated active power consumed by the different classes of RUs, together with the total import from the main grid.

It can be observed that the power demand of connected RUs is consistently larger than RESs generation, and, therefore, the active power imported at the grid almost follows the RUs demands. The HT is charged and discharged 3 times in 3 days, with the El being used at the minimum active power when no HS is connected, and at active maximum power when a HS arrives. The El is also used to inject reactive power, contrasting the voltage drop at bus 7. On the contrary, the BESS is slightly charged and discharged, in fact the small power and capacity of the battery cannot provide sufficient effect of energy arbitrage. However, the BESS is largely used to absorb reactive power

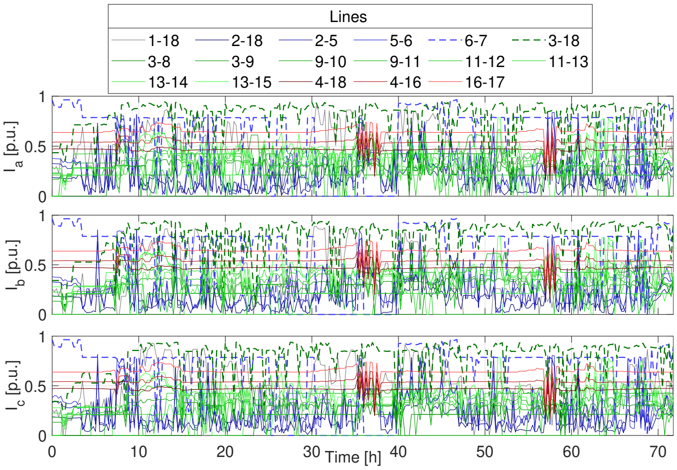

Fig. 5. Three-phase lines current expressed in p.u. on I_l^{max} basis.

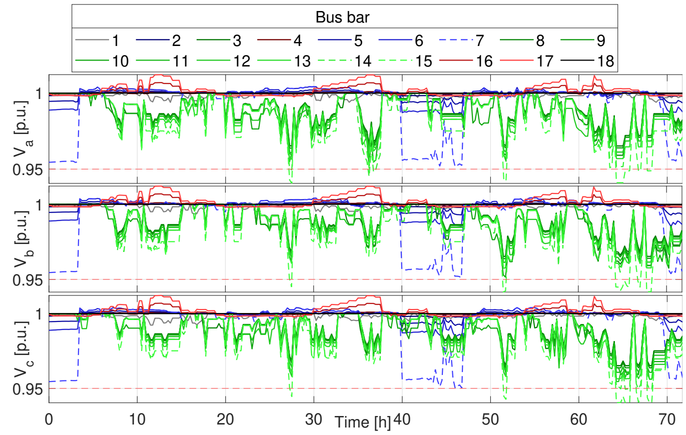

Fig. 7. Three-phase voltage amplitudes without reactive power control.

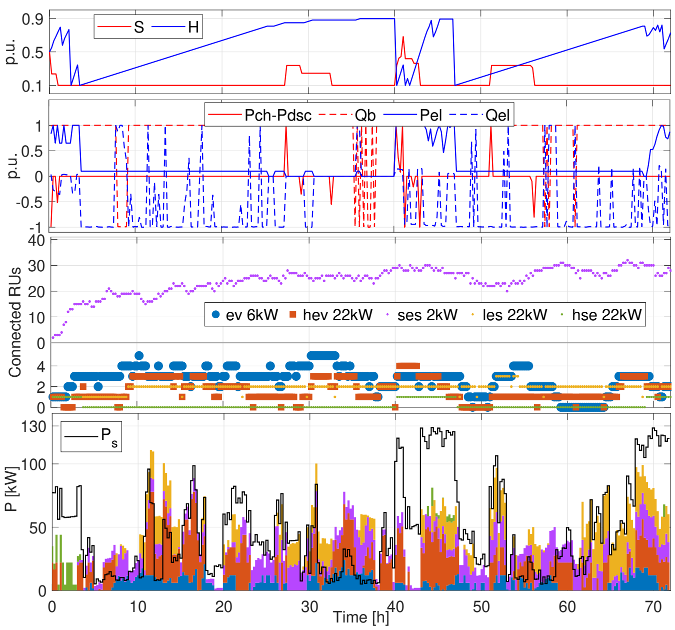

Fig. 6. From the top: BESS SoC and HT LoH; BESS and El active and reactive powers; number of connected RUs; active powers of connected RUs and total active power imported from the utility grid.

at bus 18, contrasting the effect of large PV injection and maintaining the voltage between limits.

Finally, Fig. 7 shows voltage amplitudes when operations are run without tacking into account security constraints (*i.e.* only active powers are controlled). The voltage at buses 14 and 15, hosting SESs and LESs units, respectively, falls repeatedly below 0.95 p.u., thus proving the necessity of including the grid model and security constraints in the control model.

VI. Conclusions

This work introduced an MPC-based framework that coordinates diverse onshore resources in a smart marina while enforcing grid-security constraints. By embedding a linearized power flow model into a mixed integer linear programming formulation, the controller simultaneously schedules renewable generation, storage units, and heterogeneous rechargeable loads without violating voltage or line-loading limits.

Simulation results based on the real port of Finale Ligure reveal several insights. First, neglecting network constraints leads to recurrent undervoltages at buses with concentrated electric-ship charging; incorporating voltage and current limits eliminates these violations and prevents branch overloads even under high demand. Second, although the BESS has limited energy capacity, its reactive-power capability plays a critical role in maintaining voltage profiles. Third, the electrolyzer exhibits a dual function: it satisfies hydrogen demand while providing both active and reactive support during stressed conditions.

Overall, the controller successfully tracks users' charging requirements, minimizes RES curtailment, and ensures the secure operation of the LV marina grid.

References

[1] B. Behdani, "Port 4.0: a conceptual model for smart port digitalization," *Transportation Research Procedia*, vol. 74, pp. 346–353, 2023.

[2] B. Belmoukari, J.-F. Audy, and P. Forget, "Smart port: a systematic literature review," *European Transport Research Review*, vol. 15, no. 1, p. 4, 2023.

[3] Y. Pu, W. Chen, R. Zhang, and H. Liu, "Optimal operation strategy of port integrated energy system considering demand response," in *2020 IEEE 4th Conference on Energy Internet and Energy System Integration (EI2)*, 2020, pp. 518–523.

[4] K. Qian, C. Zhou, M. Allan, and Y. Yuan, "Modeling of load demand due to ev battery charging in distribution systems," *IEEE Trans. Power Syst.*, vol. 26, no. 2, pp. 802–810, 2011.

[5] W. Wang, Q. Huo, Q. Liu, J. Ni, J. Zhu, and T. Wei, "Energy optimal dispatching of ports multi-energy integrated system considering optimal carbon flow," *IEEE Trans. Intell. Transp. Syst.*, 2023.

[6] Q. Zhang, Q. Shan, and T. Li, "Large port energy management based on distributed optimization," in *International Conference on Information, Cybernetics, and Computational Social Systems*, 2020, pp. 108–113.

[7] A. Garces, "A linear three-phase load flow for power distribution systems," *IEEE Trans. Power Syst.*, vol. 31, no. 1, pp. 827–828, 2016.

[8] M. Crosa, F. D'Agostino, S. Massucco, P. Pongiglione, M. Saviozzi, and F. Silvestro, "The podcast project: An application of volt/var optimization to the electric distribution network of sanremo (italy)," in *2019 1st International Conference on Energy Transition in the Mediterranean Area (SyNERGY MED)*, 2019, pp. 1–6.

979-8-3315-8138-1